in spatial regions close to the metal—one might even say, if the chromophore is "intrinsically" chiral—as argued here in terms of misdirected valency, this interdependence of parametrization and interpretation seems especially apt. On the other hand, in systems—which are not at all exemplified by the present study—where chirality appears to be sourced in rather distant structures—in the "second" coordination shell or even within a chiral solvent (as in DICD studies, for example)—and where a "through-space" rather than a "through-bond" mechanism carries most credence, the present approach is likely to be less appropriate and probably less successful. We must emphasize once more, therefore, that the approach here is part of a ligand-field scheme in which parameters refer directly to orbital admixtures into the *d* basis—and thence parametrized within effective operators. Formalistically, no doubt, distantly sourced, "through-space" perturbations could be included within such effective operators but only if the sort of local restrictions we adopt are withdrawn and then, of course, with a consequent loss of local (inner coordination shell) chemical correlation.

The internal consistency of the model with respect to the magnitudes (point ii) of the *e* and *t* parameters is also encouraging. For example, the $e_\sigma$(Cl) and $e_\sigma$(N) values for the three chromophores, as listed in Table I, uniformly indicate somewhat better amine $\sigma$ donation than chlorine. The $e_\pi$(Cl) values also show a consistent pattern that accords well with experience.[5,9] While the magnitudes of the remaining *e* and *t* parameters are somewhat uncertain in view of the correlations discussed earlier, they are consistent throughout the series; not least in that $^Pt$ contributions appear to be larger than $^Ft$ for both $\sigma$ and $\pi$ interactions and for Co–N and Co–Cl ligations.

**Acknowledgment**. N.D.F. thanks the SERC for a Research Studentship.

Contribution from the University Chemical Laboratory, Lensfield Road, Cambridge CB2 1EW, U.K.

# Energies, Intensities, and Circular Dichroism of d–d Transitions in Trigonal-Bipyramidal Cobalt(II) and Nickel(II) Chromophores†

Neil D. Fenton and Malcolm Gerloch*

*Received July 11, 1989*

The energies, electric-dipole absorbances, and rotatory strengths of "d–d" transitions in a series of nominally trigonal-bipyramidal chromophores have been reproduced quantitatively within the cellular ligand-field (CLF) approach. The series comprise M(*S*-tan)X with M = Co(II) or Ni(II), X = NCS, Cl, Br, or I, and *S*-tan is the tripodal triamine $Me_2NCH_2CH(Me)N(CH_2CH_2NMe_2)_2$. Separate analyses of the three spectral properties have established CLF energy parameters, $e_\lambda$, and electric-dipole transition moment parameters, $^Lt_\lambda$, that describe a consistent pattern of electron distribution throughout the series. It is argued that the circular dichroism, originating in the $\delta\delta\delta$ conformation of the tripodal ligand, arises through slight bent bonding between the equatorial amines and the central metal. This misdirected valency is monitored with small values of the local $e_{\pi\sigma}$ CLF parameters or by small values of $^Lt_\pi$ parameters for the equatorial ligations.

## Introduction

In 1985, Utsuno et al.[1] described the synthesis and characterization by X-ray crystallography and electronic spectroscopy of a series of trigonal bipyramidal complexes incorporating a new tripodal tetraamine, *S*-tan. The ligand *S*-tan, $Me_2NCH_2CH(Me)N(CH_2CH_2NMe_2)_2$, which closely resembles the tripod $Me_6tren$, $N(CH_2CH_2NMe_2)_3$, adopts a chiral conformation within the complex ions $[M(S\text{-tan})X]^{n+}$ for M = Co(II) or Ni(II) and X = $NCS^-$, $Cl^-$, $Br^-$ or $I^-$ among others. Utsuno et al. reported absorption and circular dichroism (CD) spectra for the "d–d" transitions in all members of these series of complexes and discussed the qualitative features of the CD spectra in terms of selection rules for electric and magnetic dipole moments under $C_{3v}$ symmetry. As part of a program to extend the reach of ligand-field analysis, we report here on the *quantitative* reproduction of both absorption and rotatory strengths in these complexes.

Computation of the absorption intensities requires an evaluation of electric-dipole matrix elements: these, together with magnetic-dipole elements, are needed for a calculation[2] of the rotatory strengths provided by the CD experiment. Ligand-field theory in general and our recent extensions[3-5] of it in particular offer means of expressing both electric- and magnetic-dipole matrices within the same d-function basis that is conventionally employed in the calculation of transition energies. Inevitably, in view of the very great difficulty in implementing any satisfactory ab initio calculation of ligand-field properties throughout the transition series, the approach is parametric. A parametrization scheme may have utility beyond the mere reproduction of observables, however difficult that often is, only if it is defined directly in terms of physically comprehensible quantities. To date, the best parametrization structures by this criterion are those exploiting a principle of spatial superposition rather than of a global multipole expansion. Contact with chemical bonding and structure is minimal when the $10Dq$ or $\Delta_{oct}$ parameters of the global (molecular) decomposition of a ligand field are used and is even less for molecules with little or no symmetry. On the other hand, the separation of $\sigma$- and $\pi$-bonding factors from each individual ligand in a complex, as first effected within the angular overlap model (AOM)[6,7] but subsequently and more properly within the cellular ligand-field (CLF) model,[3,8,9] has brought to ligand-field analysis the familiar notion of the functional group, together with interpretations—and hence exploitations—of all ligand-field properties that are made by using mainstream chemical vocabulary. Furthermore, necessary approximations and assumptions

† No reprints available from this laboratory.

(1) Utsuno, S.; Miyamae, H.; Horikoshi, S.; Endo, I. *Inorg. Chem.* **1985**, *24*, 1348.
(2) Schellman, J. A. *Chem. Rev.* **1975**, *75*, 323.
(3) Gerloch, M. *Magnetism & Ligand-Field Analysis*; Cambridge University Press: Cambridge, England, 1983.
(4) Gerloch, M.; McMeeking, R. F. *J. Chem. Soc., Dalton Trans.* **1975**, 2443.
(5) Brown, C. A.; Gerloch, M.; McMeeking, R. F. *Mol. Phys.* **1988**, *64*, 771.
(6) Schäffer, C. E. *Struct. Bonding* **1968**, *5*, 68.
(7) Schäffer, C. E.; Jørgensen, C. K. *J. Inorg. Nucl. Chem.* **1958**, *8*, 143.
(8) Gerloch, M. In *Understanding Molecular Properties*; Avery, J. S.; Dahl, J.-P., Hansen, A., Eds.; Reidel: Dordrecht, The Netherlands, 1987; p 111.
(9) Woolley, R. G. *Int. Rev. Phys. Chem.* **1987**, *6*, 93.

0020-1669/90/1329-3726$02.50/0 

**Table I.** Structural Parameters for Tripod Ligands[a]

| metal | tripod | X | $\bar{a}$ | $b$ | $c$ | $\bar{\alpha}$ | $\bar{\beta}$ | $\bar{\gamma}$ | $\bar{\delta}$ | $\bar{\epsilon}$ | $\Delta$ |
|---|---|---|---|---|---|---|---|---|---|---|---|
| Co | $Me_6$tren | Br | 2.08 | 2.15 | 2.43 | 81.1 | 98.9 | 109.3 | 109.3 | 117.6 | 0.32 |
| | *S*-tan | NCS | 2.13 | 2.20 | 1.99 | 82.0 | 98.0 | 108.0 | 108.0 | 118.1 | 0.30 |
| Ni | $Me_6$tren | Br | 2.13 | 2.10 | 2.47 | 84.2 | 95.8 | 104.0 | 107.7 | 119.0 | 0.22 |
| | $Me_6$tren | NCS | 2.10 | 2.04 | 1.97 | 85.4 | 95.3 | 103.9 | 109.4 | 119.2 | 0.22 |
| | $Me_6$tren | I | 2.13 | 2.10 | 2.67 | 84.2 | 95.8 | 104.0 | 107.7 | 119.0 | 0.22 |
| Cu | $Me_6$tren | Br | 2.14 | 2.07 | 2.39 | 84.7 | 96.3 | 104.0 | 108.0 | 119.1 | 0.20 |
| | tren | NCS | 2.10 | 2.04 | 1.95 | 84.7 | 96.0 | 108.4 | 108.3 | 119.0 | 0.17 |

[a] Refer to Figure 1. Bond lengths are in angstroms; angles are in degrees. Bar over a symbol refers to the mean of three quantities related by exact or *pseudo* 3-fold axis.

that may be required for reasons of tractability are, so far as possible, expressible directly in terms of structure and chemical bonding instead of algebra.

One such group of assumptions made within AOM and CLF models is that local ligand-field potentials may be taken as diagonal with respect to a metal–ligand axis frame defined by the local electron-density distribution. For ligations with approximate $C_{2v}$ or higher *pseudo*symmetry, parametrization with local $e_\sigma$, $e_{\pi x}$ and $e_{\pi y}$ variables has repeatedly proved entirely satisfactory. With lower local symmetry, however, explicit recognition of the non-diagonal nature of bent bonding, for example, has proved necessary.[10-16] Inclusion of nonzero $e_{\pi\sigma}$ parameters into the modeling of such fine detail is physically obvious in a way that the addition of local $Y_1^2$ and $Y_1^4$ harmonics into the multipole expansions of the local field, let alone of general addition to the $Y_q^k$ of the global potential, is not.

The appeal of the cellular parameterization of ligand-field energies with the $\{e_\lambda\}$ variables has led to the development of a ligand-field modeling[5] of "d–d" spectral intensities using cellular $\{^Lt_\lambda\}$ parameters. From some score of quantitatively successful reproductions of experimental chromophore "d–d" intensities—in both polarized and unpolarized light—empirical and theoretical understanding of the bonding significance of these local $t$ parameters is emerging.[5,14-19] Taken together, common views of the detailed nature of the bonding in transition-metal complexes arise from spectral frequencies, magnetic susceptibilities, and ESR $g$ values via the energy parameter set, $\{e\}$, and from spectral intensities via the effective eigenvector parametrization, $\{t\}$. Of late, the second group of properties has been extended[16] to include the differential intensities of optical activity. The present study is the second such to exploit the spatial superposition of the cellular ligand-field approach together with this wide range of experimental data.

## Coordination Geometry

The coordination geometry of the nominally trigonal-bipyramidal cations $[MXL]^{n+}$, L = $Me_6$tren or *S*-tan, is shown schematically in Figure 1. While full X-ray cyrstallographic analyses have been completed for several $Me_6$tren complexes, only one member of the *S*-tan series has been so defined,[1] viz [Co(NCS)(*S*-tan)]$ClO_4$. Relevant structural parameters[20] for this and members of the $Me_6$tren and tren series are collected in Table I. Comments in two areas are appropriate at this stage.

Consider first the patterns of axial and equatorial M–N bond lengths. We have discussed elsewhere[13,14,20] the trend ax > eq for $d^7$ to ax < eq for $d^9$ in terms of two factors: increasing effective nuclear charge on the metal on traversing the transition series from

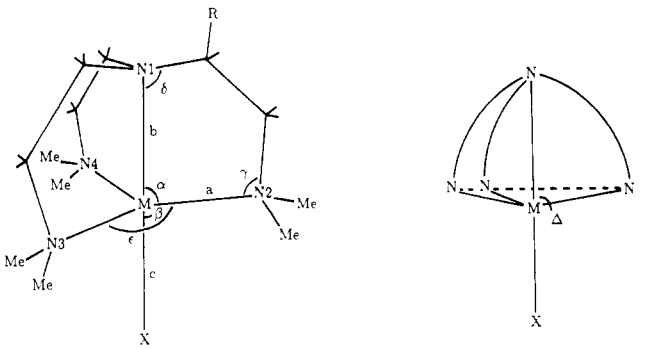


**Figure 1.** Trigonal-bipyramidal geometry of *S*-tan and tren complexes. See Table I. R = Me for *S*-tan; R = H for $Me_6$tren.

cobalt(II) to copper(II) tending to decrease all M–N bond lengths and the filling of the $d_{xy}/d_{x^2-y^2}$ orbitals along that series so increasingly frustrating bonding with the equatorial amine set.

Secondly, we observe that the displacement, $\Delta$, of the metal atom below the plane of the three equatorial nitrogen donors is some 0.3 Å for cobalt species and 0.2 Å for the nickel. The angles $N_{ax}$–M–$N_{eq}$ ($\alpha$) reflect this same feature. It is this angular variation rather than that of the bond lengths above which is crucial in the ligand-field analyses that follow. Thus it is desirable, wherever possible, to base each analysis upon a precisely known molecular geometry. As this is only possible in the present *S*-tan series for the [Co(NCS)(*S*-tan)]$^+$ chromophore, we must rely on some degree of isostructuralism for the rest. Bond length variations are of no concern here, of course, for they are subsumed within the $e$ or $t$ parameter values. Angular variations, however, are not. We have considered, therefore, two detailed geometries: one defined by the explicit structural analysis of [Co(NCS)(*S*-tan)]$ClO_4$, and the other defined in the same way but with the metal atom moved 0.1 Å closer to the equatorial amine plane.

## Transition Energies

We have carried out ligand-field analyses only on the halo and thiocyanato complexes of cobalt(II) and nickel(II) within these series as these offer the best ratios of observables to parameters. As usual more transitions are observed for the $d^7$ and $d^8$ species than for $d^9$. This is especially true for the CD spectra discussed later. In addition to the Racah $B$ parameter for interelectron repulsion and the spin–orbit coupling coefficient, $\zeta$, we represent the cellular ligand fields with $e_\sigma$(eq) for the equatorial amines of the *S*-tan tripod, and $e_\sigma$(ax) and $e_\pi$(X) for the mean $\sigma$ interactions of the axial amine and nontripod ligand and for the $\pi$ ligation of the latter, respectively.

Calculations, made by using our CAMMAG3 program suite,[21] were performed within the maximum-spin, free-ion terms: $^4F + {}^4P$ for $d^7$ and $^3F + {}^3P$ for $d^8$. Final checks were made by using the full $d^7$ and $d^8$ bases, but no significant differences were observed. Three-part analyses have addressed the reproduction of transition energies, absorption intensities, and rotatory strengths, essentially in that order. First we report the energy studies.

These began with the [Co(NCS)(*S*-tan)]$^+$ chromophore as the only member of these series with a precisely known coordination

(10) Deeth, R. J.; Duer, M. J.; Gerloch, M. *Inorg. Chem.* **1987**, *26*, 2573.
(11) Deeth, R. J.; Duer, M. J.; Gerloch, M. *Inorg. Chem.* **1987**, *26*, 2579.
(12) Deeth, R. J.; Gerloch, M. *Inorg. Chem.* **1987**, *26*, 2583.
(13) Fenton, N. D.; Gerloch, M. *Inorg. Chem.* **1987**, *26*, 3273.
(14) Fenton, N. D.; Gerloch, M. *Inorg. Chem.* **1989**, *28*, 2975.
(15) Duer, M. J.; Gerloch, M. *Inorg. Chem.* **1989**, *28*, 4260.
(16) Fenton, N. D.; Gerloch, M. *Inorg. Chem.*, previous paper in the issue.
(17) Brown, C. A.; Duer, M. J.; Gerloch, M.; McMeeking, R. F. *Mol. Phys.* **1988**, *64*, 793.
(18) Brown, C. A.; Duer, M. J.; Gerloch, M.; McMeeking, R. F. *Mol. Phys.* **1988**, *64*, 825.
(19) Duer, M. J.; Gerloch, M. *J. Chem. Soc., Dalton Trans.* **1989**, 2109.
(20) Deeth, R. J.; Gerloch, M. *Inorg. Chem.* **1985**, *24*, 4490 and references therein.
(21) Dale, A. R.; Duer, M. J.; Fenton, N. D.; Gerloch, M.; McMeeking, R. F. CAMMAG3, a FORTRAN program suite.

**Table II.** Ligand-Field Energy Parameters ($cm^{-1}$) Yielding Optimal Reproduction of Transition Energies for MLX (M = Co(II), Ni(II); L = *S*-tan; X = NCS, Cl, Br, I)

| | CoLNCS | CoLCl | CoLBr | CoLI |
|---|---|---|---|---|
| $e_\sigma(eq)^d$ | 3700[e] | 3800 | 3900 | 4100 |
| $\bar{e}_\sigma(ax)^d$ | 4650 | 4300 | 4100 | 3800 |
| $e_\pi(X)$ | 1000 | 1200 | 1250 | 1250 |
| $B$ | 780 | 750 | 740 | 730 |
| $\sum^b$ | 22400 | 22400 | 22400 | 22400 |
| $\zeta^c$ | 450 | 450 | 450 | 450 |
| | **NiLNCS** | **NiLCl** | **NiLBr** | **NiLI** |
| $e_\sigma(eq)^d$ | 3500 | 3500 | 3600 | 3700 |
| $\bar{e}_\sigma(ax)^a$ | 5300 | 5050 | 4900 | 4700 |
| $e_\pi(X)$ | 700 | 900 | 900 | 950 |
| $B$ | 880 | 850 | 830 | 805 |
| $\sum^b$ | 22400 | 22400 | 22400 | 22400 |
| $\zeta^c$ | 550 | 550 | 550 | 550 |

[a] Mean of $e_\sigma$(amine) and $e_\sigma(X)$. [b] $\sum \equiv \sum_i^N(e_\sigma + e_{\pi x} + e_{\pi y})_i$ for $N$ = 5 ligators. Fixed value—see text. [c] Fixed values. [d] $e_\sigma(eq)$ and $e_\pi(ax)$ values suffer correlation—see text. [e] Estimated errors are as follows: for $\bar{e}_\sigma(ax)$, ±100 $cm^{-1}$; for $e_\sigma(eq)$ and $e_\pi(X)$, ±100 $cm^{-1}$ relative to correlation; for $B$, ±20 $cm^{-1}$.

geometry. Wide variations of all parameter values were made, and as observed in similar analyses[20] of the analogous $Me_6$tren complexes, good reproduction of experimental transition energies is achieved but not uniquely. Best fits are obtained throughout a somewhat extended region of polyparameter space that is principally characterized by correlation between $e_\pi(X)$ and $e_\sigma(eq)$. The correlated region is bounded at its ends, undoubtedly because of the inexact 3-fold symmetry of the chromophore. On the other hand, the large range of the correlation, as indicated by the values $e_\pi(X)$ = 600 $cm^{-1}$ with $e_\sigma(eq)$ = 3600 $cm^{-1}$ to $e_\pi(X)$ = 1500 $cm^{-1}$ with $e_\sigma(eq)$ = 4000 $cm^{-1}$, reflects the smallness of those departures from axial symmetry. The ligand-field trace,[12,22-25] $\Sigma$, given by the sum of all local diagonal $e_\lambda$ parameters, varies continuously throughout the "best-fit" region, with values 21 200 and 24 250 $cm^{-1}$ corresponding to the parameter pairs above. Wide experience of trace values for four-, five- and six-coordinate complexes of $d^6$ to $d^9$ metal(II) complexes has determined[22,24] an essentially constant value for $\Sigma$ of ca. 22 000 $cm^{-1}$. The optimal parameter values presented in Table II have been chosen from the correlated best-fit region to give that same value of the trace. The quality of reproduction of the experimental transition energies is shown in Table III.

Similar analyses of the halo analogues, $[Co(NCS)X]^+$ (X = Cl, Br, I), were undertaken with use of the same angular coordination geometry. Any bond length variations are, of course, unimportant, being subsumed within the parameter values. In each case, excellent reproduction of all "d–d" transition energies was achieved, though again for a correlated region of parameter space which closely parallels that found for the thiocyanate chromophore. As before, optimal parameter sets, presented in Table II, have been selected to yield ligand-field traces of ca. 22 000 $cm^{-1}$. The corresponding agreements between observed and calculated transition energies are included in Table III.

When a similar strategy was adopted for analyses of the nickel species, no choice of parameter values whatsoever afforded satisfactory reproduction of experimental transition energies. These failures were all characterized by the placing of one transition at ca. 12 000 $cm^{-1}$ instead of at ca. 14 000–15 000 $cm^{-1}$, as observed. However, adoption of the modified angular geometry resulting from the displacement of the nickel atom 0.1 Å nearer to the equatorial amine plane, as described above, resolved the problem completely for all four nickel chromophores. "Best-fit" parameter values are correlated again, but within these regions, reproduction of all transition energies is good, as shown in Table IV for the optimal parameter sets in Table II chosen once more for trace values of ca. 22 000 $cm^{-1}$.

### The Energy Parameters

The optimal parameter sets collected in Table II describe consistently comprehensible trends. For each of the cobalt and nickel series, we observe $e_\sigma(ax)$, being the average of $e_\sigma$ values for the axial amine and the halogen or thiocyanate, to decrease smoothly along the series NCS > Cl > Br > I reflecting the decreasing $\sigma$ donor strengths of these ligands in the spectrochemical series. Electroneutrality of the central metal tends to be maintained by a corresponding increase in the $\sigma$ donor strengths of the equatorial amines along the same series: the increases are more modest, presumably because there are three such equatorial amines to compensate the metal for the changes imposed by the halogen or *pseudo*halogen group. At the same time, we note the small increase, or near constancy, in $\pi$ donation from the X group along the series. This we take to reflect the operation of the electroneutrality principle on the X group, in that smaller $\sigma$ donation will tend to encourage greater $\pi$ donation. This factor will be offset to some extent, of course, by the increasing M–X bond lengths and greater orbital diffuseness along the series.

We have commented above, and elsewhere,[20] upon the changing pattern of axial versus equatorial metal–amine bond lengths along the transition-metal series. In the strong-field limit, the d-orbital configurations for ions in trigonal-bipyramidal coordination are $(d_{xz,yz})^4(d_{xy,x^2-y^2})^2(d_{z^2})^1$ for $d^7$ and $(d_{xz,yz})^4(d_{xy,x^2-y^2})^3(d_{z^2})^1$ for $d^8$. The increasing occupancy of the equatorial orbitals frustrates ligation with the equatorial amines more in the nickel complexes than in the cobalt complexes. However, the general increase in effective nuclear charge as one traverses the periodic table from left to right combines with this factor to yield the overall trend that axial bonding increases in strength as cobalt is replaced by nickel. The bond lengths in Table I reflect this trend, as do ligand-field parameters in a series of $Me_6$tren complexes with the present geometry. The $e_\sigma(ax)$ values in Table II similarly confirm this bonding trend, as indeed do the slightly reduced values of $e_\sigma(eq)$. Further confirmation of this view and of the proposal in the preceding paragraph concerning the operation of the electroneutrality principle on the X groups derives from the smaller $e_\pi(X)$ parameter values determined for the nickel complexes as compared with the cobalt. Thus, we see the increased $\sigma$ donation of X toward nickel relative to cobalt accompanied by a decreased $\pi$ donation.

Finally, the smooth decrease in interelectron repulsion energy, as monitored by the Racah $B$ parameters, along the series NCS > Cl > Br > I accords well with the nephelauxetic series and generally increases confidence in these ligand-field analyses. It is possible that an increasing nephelauxetic effect, reflecting increased donation from the ligand set as a whole, should be accompanied by decreasing values of the ligand-field trace, $\Sigma$. If so, selecting different points along the $e_\pi(X)/e_\sigma(eq)$ correlations in the ligand-field analyses so as to produce smaller $\Sigma$ values decreases both $e_\pi(X)$ and $e_\sigma(eq)$ values somewhat. Neither the trends in Table II nor the interpretations of them would be greatly affected by such changes. Overall, therefore, we consider these eight, essentially independent, energy analyses to provide a robust illustration of the quality of contemporary ligand-field study.

### Absorption Intensities

Intensities of the transitions in all eight complexes were estimated, as in the first applications[17,18] of the CLF model for intensities, as integrated areas under the reported spectral traces by cutting out paper copies and weighing. Deconvolutions were attempted only for well-resolved bands so that four band intensities were so determined for each of the cobalt chromophores and four for each nickel. Band limits are shown in Figure 2.

Intensity computations within our CLF model are predicated upon the ligand fields established by the preceding energy analyses, in particular, upon the ligand-field potentials so determined. Although, for each chromophore, we take those fields corresponding to the parameter sets in Table II, we note that the multipole expansion of the nonspherical parts of the potentials vary very little along the $e_\pi(ax)/e_\sigma(eq)$ correlations described. In

(22) Deeth, R. J.; Gerloch, M. *Inorg. Chem.* **1985**, *24*, 1754.
(23) Woolley, R. G. *Chem. Phys. Lett.* **1985**, *118*, 207.
(24) Deeth, R. J.; Gerloch, M. *J. Chem. Soc., Dalton Trans.* **1986**, 1531.
(25) Fenton, N. D.; Gerloch, M. *J. Chem. Soc., Dalton Trans.* **1988**, 2201.

**Table III.** Comparisons between Observed Transition Energies ($cm^{-1}$) and Those Calculated[a] with the Optimal Parameter Sets of Table II, for Co(*S*-tan)X

| | NCS | | Cl | | Br | | I | |
|---|---|---|---|---|---|---|---|---|
| band[b] | obsd | calcd | obsd | calcd | obsd | calcd | obsd | calcd |
| 1 | 20400 | 20488<br>20168 | 20000 | 19468<br>19149 | 19000 | 19053<br>18735 | 18300 | 18586<br>18270 |
| 2 | 16300 | 16453 | 16100 | 15942 | 16200 | 15918 | 16200 | 16149 |
| 3 | 13300 | 13854<br>13240 | 12500 | 13012<br>12399 | 12300 | 12692<br>12081 | 12100 | 12402<br>11793 |
| 4 | 5600 | 5532<br>5150<br>4499 | 5600 | 5389<br>5011<br>4530 | 5600 | 5385<br>5012<br>4610 | 5400 | 5466<br>5112<br>4790 |
| | | 3134 | | 3134 | | 3222 | | 3425 |
| | | 0 | | 0 | | 0 | | 0 |

[a] Averaged over spin quartets. [b] Band limits shown in Figure 2.

**Table IV.** Comparisons between Observed Transition Energies ($cm^{-1}$) and Those Calculated[a] with the Optimal Parameter Sets of Table II, for Ni(*S*-tan)X

| | NCS | | Cl | | Br | | I | |
|---|---|---|---|---|---|---|---|---|
| band[b] | obsd | calcd | obsd | calcd | obsd | calcd | obsd | calcd |
| 1 | 24300<br>ca. 21000 | 24275<br>21714<br>21305 | 23200<br>ca. 20000 | 23193<br>20753<br>20345 | 22700<br>ca. 19500 | 22671<br>20351<br>19941 | 22100<br>ca. 19500 | 21943<br>19762<br>19350 |
| 2 | 15500 | 14979 | 14600 | 14250 | 14100 | 14062 | 13600 | 13716 |
| 3 | 12400 | 12923<br>11548 | 10600 | 12223<br>10845 | 10400 | 11990<br>10587 | 10100 | 11606<br>10179 |
| 4 | 7500 | 7636<br>7268 | 7000 | 7256<br>6896 | 7100 | 7244<br>6886 | 7100 | 7146<br>6792 |
| | | 770 | | 769 | | 771 | | 774 |
| | | 0 | | 0 | | 0 | | 0 |

[a] Averaged over spin-triplet components. [b] Band limits shown in Figure 2.

**Table V.** Optimal Intensity Parameters[a] Reproducing "d–d" Band Intensities for M(*S*-tan)X (M = Co, Ni; X = NCS, Cl, Br, I)

| | Co | | | | Ni | | | |
|---|---|---|---|---|---|---|---|---|
| | NCS | Cl | Br | I | NCS | Cl | Br | I |
| $^{P}t_{\sigma}$(ax) | 0 (5)[b] | −92 (10) | −70 (10) | −83 (10) | 34 (3) | −26 (3) | −36 (5) | −37 (5) |
| $^{F}t_{\sigma}$(ax) | 43 (5) | −92 (10) | −70 (10) | −83 (10) | 86 (10) | −26 (3) | −36 (5) | −37 (5) |
| $^{P}t_{\pi}$(X) | 16 (5) | 0 (5) | 7 (3) | 0 (3) | 17 (5) | 0 (5) | 7 (5) | 0 (5) |
| $^{F}t_{\pi}$(X) | 8 (5) | 12 (5) | 7 (3) | 16 (3) | 17 (5) | 0 (5) | 0 (5) | 0 (5) |
| $^{P}t_{\sigma}$(Neq) | 0 (5) | 0 (5) | 0 (5) | 0 (5) | 5 (5) | 0 (5) | 0 (5) | 0 (5) |
| $^{F}t_{\sigma}$(Neq) | 11 (5) | 12 (5) | 14 (5) | 16 (5) | 34 (5 | 34 (5) | 36 (5) | 37 (7) |

[a] $^{L}t_{\lambda}/10^{-20}$ D. [b] Estimated errors in parentheses.

short, the ambiguities in describing the ligand-field potentials at the cellular level do not carry over to the global or molecular regime. (Similar circumstances, which need not, and do not, occur in general, have been observed and exploited in previous intensity analyses.[17]) Consequently, the assumption that $\Sigma \approx 22\,000$ $cm^{-1}$ is not crucial to the ensuing intensity studies.

The intensity analyses for all eight chromophores were conducted independently but followed very similar paths and produced similar results. We report them en bloc. The parameter sets comprised $^{P}t_{\sigma}$(eq) and $^{F}t_{\sigma}$(eq) for the equatorial amine ligations; $^{P}t_{\sigma}$(ax) and $^{F}t_{\sigma}$(ax) for the axial ligations, defined as the *difference*, ax = (X − amine); and $^{P}t_{\pi}(X)$, $^{F}t_{\pi}$(X) for the halogen or thiocyanate ligations. Thus, six $^{L}t_{\lambda}$ intensity parameters were varied for each chromophore to reproduce only four observed band areas. From the outset, therefore, correlations were to be expected. The situation is improved to some extent, however, by requiring acceptable reproduction of the partly resolved components of $\rightarrow {}^{3,4}P$ transitions. Further, the following analyses of rotatory strengths support the results of the absorption strength analyses we now describe.

As much experimental intensity data is reported on arbitrary scales, the parameter structure of our model has been designed to reproduce intensity distributions, that is, relative intensities. Accordingly, one parameter, initially empirically determined as relatively important, is held fixed, so reducing the variable set by one. When, as here, absolute absorption strengths are known, the parameter set that reproduces an intensity distribution is subsequently scaled to experiment. The overall degree of parametrization is thus reinstated. Nevertheless, each analysis proceeds by first fixing one $t$ parameter and seeking a reproduction of the relative intensity pattern.

**Table VI.** Comparisons between Observed Intensities[a] and Those Calculated with the Parameter Sets of Tables II and V for the Co(*S*-tan)X Chromophores

| | NCS | | Cl | | Br | | I | |
|---|---|---|---|---|---|---|---|---|
| band | obsd | calcd | obsd | calcd | obsd | calcd | obsd | calcd |
| 1 | 86 | 81 | 95 | 101 | 87 | 78 | 82 | 76 |
| 2 | 117 | 115 | 41 | 43 | 53 | 55 | 74 | 76 |
| 3 | 34 | 44 | 27 | 25 | 28 | 32 | 26 | 28 |
| 4 | 23 | 21 | 14 | 9 | 21 | 23 | 18 | 20 |

[a] $D_{gn}\nu_{gn}/10^{-35}$ $D^2$ for transition $g \rightarrow n$ with frequency $\nu_{gn}$, summed over band components.

Relative to $^{F}t_{\sigma}$(ax) = 100 arbitrary units, all other $t$ parameters were varied widely and initially in steps of 10 within our standard trial-and-error exploration of parameter space. A single, but correlated, region was found to afford excellent reproduction of experimental intensity distributions for each of the eight chromophores. The correlations were between $^{P}t_{\sigma}$(ax) and $^{F}t_{\sigma}$(ax), so that these parameters are not so well determined in these analyses. All other parameter values are quite well established. Optimal parameter sets so determined are listed in Table V, after scaling to align the calculated intensity distributions with observed absolute magnitudes. Comparisons between observed and calculated intensities are made in Tables VI and VII. Note that

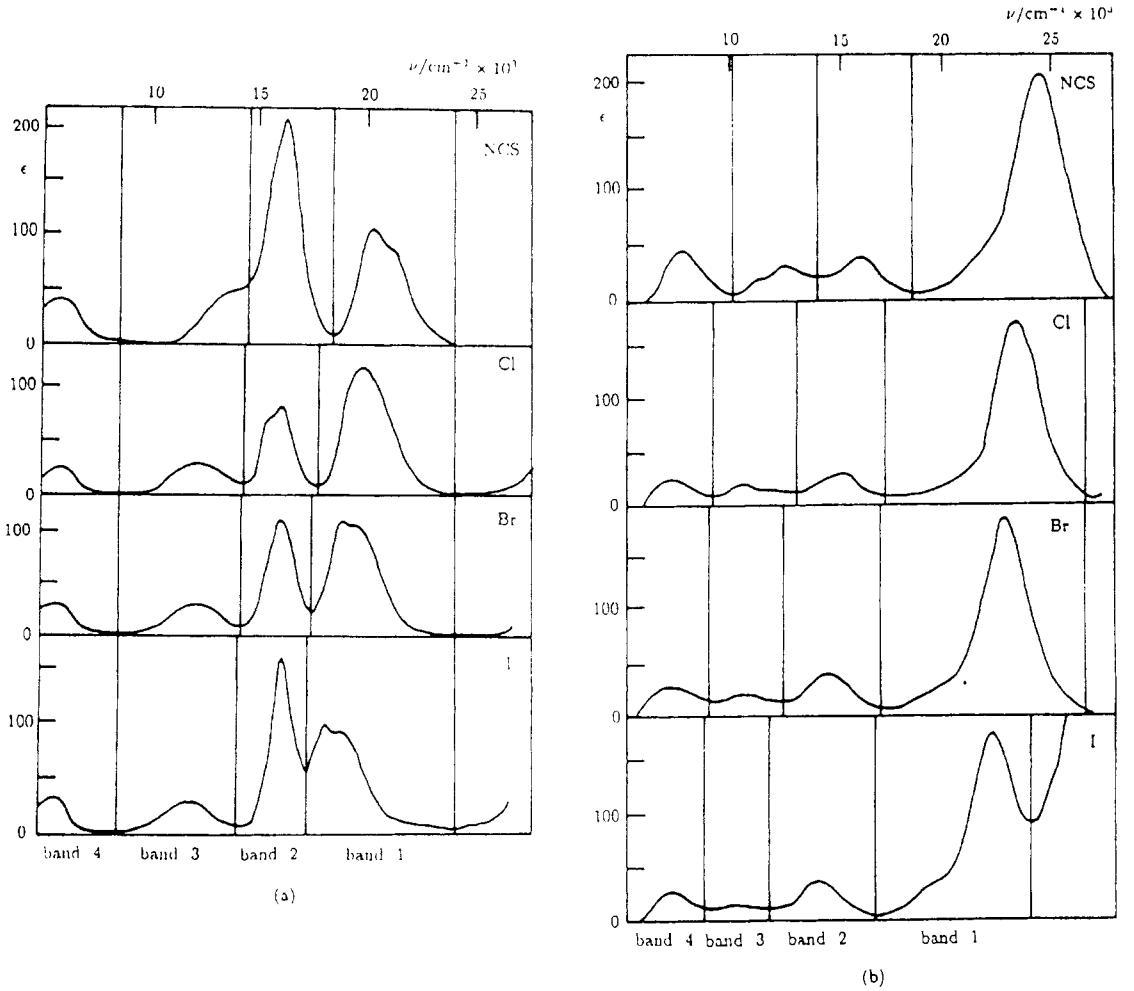


**Figure 2.** Absorption spectra[1] for the M(*S*-tan)X series: (a) M = Co; (b) M = Ni. Bands indicate limits of integration for intensity analyses.

**Table VII.** Comparisons between Observed Intensities[a] and Those Calculated for the Parameter Sets of Tables II and V for the Ni(*S*-tan)X Chromophores

| | NCS | | Cl | | Br | | I | |
|---|---|---|---|---|---|---|---|---|
| band | obsd | calcd | obsd | calcd | obsd | calcd | obsd | calcd |
| 1 | 224 | 211 | 172 | 166 | 193 | 188 | 197 | 180 |
| 2 | 34 | 44 | 28 | 28 | 35 | 38 | 38 | 38 |
| 3 | 27 | 31 | 20 | 25 | 17 | 26 | 17 | 32 |
| 4 | 31 | 20 | 20 | 15 | 23 | 21 | 20 | 17 |

[a] $D_{gn}\nu_{gn}/10^{-35}$ D² for transition $g \rightarrow n$ with frequency $\nu_{gn}$, summed over band components.

for all systems studied here, variations in the spin-orbit coupling coefficient have little effect on computed intensities: this has been discussed previously.[17]

### The Intensity Parameters

Absolute intensities for each of the eight chromophores studied here have been obtained from the solution experiments so that the optimal $t$ parameter sets in Table V are reported on the same, absolute scale. Most of our earlier intensity analyses[14-19] were based upon the relative intensities provided by crystal transmission experiments. In those cases, discussions had to be confined to comparisons between ${}^{L}t_{\lambda}$ values within each chromophore separately or between ratios of ${}^{P}t_{\lambda}$:${}^{F}t_{\lambda}$ values. Here, we consider the data whole.

First, we observe closely similar $t$ values throughout the series. That is to be expected within the nickel or within the cobalt series, of course, for the spectra are so similar. More noteworthy is the similarity of $t$ values for the complexes of the $d^7$ and $d^8$ metals. The similarity extends to the roughly homogeneous behavior of the halo complexes as a group for both metals and the contrasting behavior for each metal of the thiocyanate chromophores.

**Table VIII.** Possible $t_\sigma$ Parameters[a] for Axial Ligations in M(*S*-tan)X Species (See Text)

| | CoLNCS | CoLHa | NiLNCS | NiLHa |
|---|---|---|---|---|
| ${}^{P}t_{\sigma}$(amine) | 150 | 160 | 170 | 180 |
| ${}^{F}t_{\sigma}$(amine) | 90 | 100 | 100 | 110 |
| ${}^{P}t_{\sigma}$(X) | 150 | 70 | 204 | 164 |
| ${}^{F}t_{\sigma}$(X) | 133 | 10 | 186 | 84 |

[a] Parameter values on the same scale as in Table V. L = *S*-tan; Ha = halogen.

Second, the signs of the ${}^{L}t_{\sigma}$(ax) parameters defined the ligand-field strengths of the axial ligators in the order NCS > amine > halogen. This follows because of our definition that ${}^{L}t_{\sigma}$(ax) = (${}^{L}t_{\sigma}$(X) − ${}^{L}t_{\sigma}$(amine)) for X = NCS or halogen, together with the theoretical prediction,[18] and previous experimental verifications[14-19] that $t$ parameters take the same signs as the corresponding $e$ parameters. While this ordering of ligand $\sigma$ basicity occasions no surprise, it is worth noting that the energy analyses for the present chromophores cannot, in themselves, offer that conclusion, for the $e_\sigma$(ax) of Table II merely record the average of $e_\sigma$(amine) and $e_\sigma$(X).

The ${}^{L}t_{\sigma}$(ax) values in Table V record the differences between contributions to local transition moments from the amine and X ligations. While it is not possible to distinguish the roles played by these diametrically opposite ligations directly from the analyses, comparisons with earlier work[14-19] are at least suggestive. Thus, in Table VIII are offered ${}^{L}t_{\sigma}$ values for the individual axial ligations in these complexes—taken for thiocyanate and undifferentiated halogens by way of illustration—which are compatible with both the analytical differences in Table V and with prejudice deriving from earlier work. With regard to the latter, intensity analyses for two groups of chromophores containing metal–amine liga-

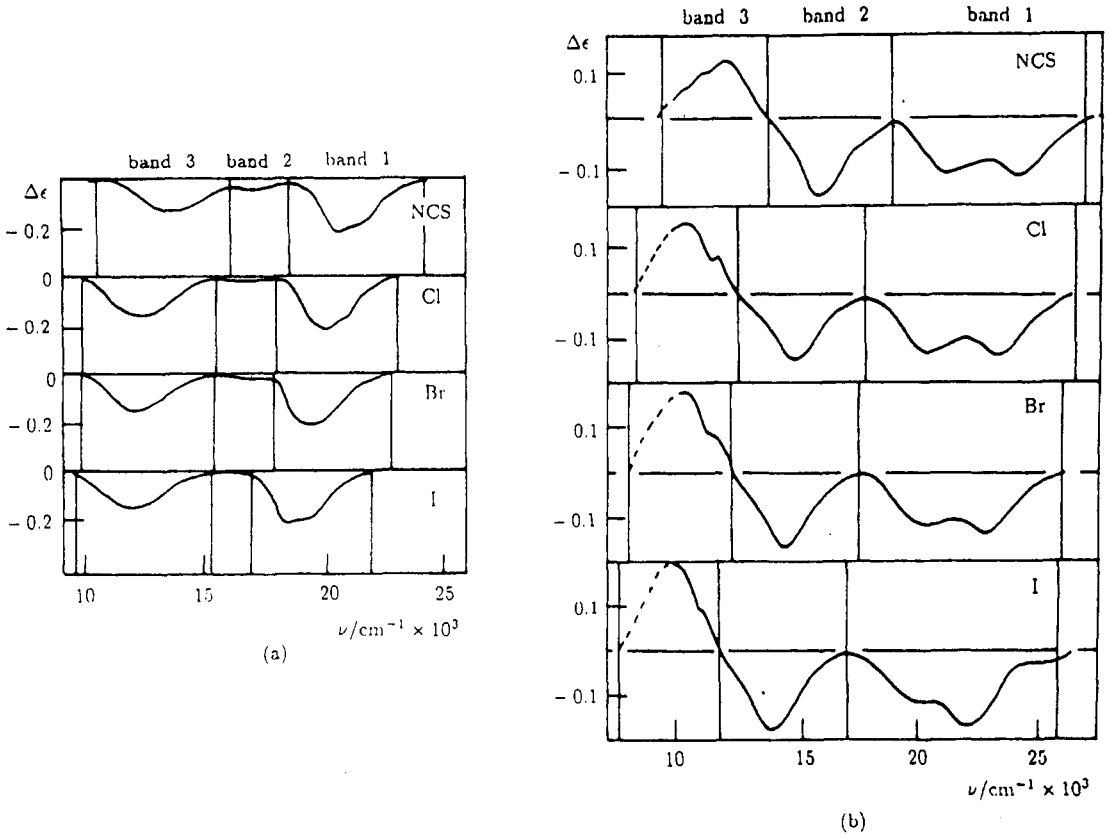


**Figure 3.** CD spectra[1] for the M(*S*-tan)X series: (a) M = Co; (b) M = Ni. Bands indicate limits of integration for analysis of rotatory strengths.

tions[16,19] have been characterized by ${}^{P}t_{\sigma} > {}^{F}t_{\sigma}$ and interpreted in terms of metal–amine bonds being quite well polarized toward the metal atoms. The values in Table VIII, which are intended to illustrate qualitative proposals, were therefore composed in three steps: (a) all ${}^{L}t_{\sigma}$ values are expected to be positive, and ${}^{F}t_{\sigma}$(amine) − ${}^{F}t_{\sigma}$(halogen) for the cobalt halo chromophores is about 90 (in the units of Table V), so establishing these values at 100 and 10 as reasonable minima; (b) the expectation that ${}^{P}t_{\sigma}$(amine) > ${}^{F}t_{\sigma}$(amine) suggested the value 160 for ${}^{P}t_{\sigma}$(amine); (c) some decrease in the ${}^{P}t_{\sigma}$(amine) value on replacing a halogen by thiocyanate, in response to the latter's greater bond strength, seems appropriate, so establishing the remaining pattern of ${}^{L}t_{\sigma}$ values in Table VIII. While these guesses only describe a possible scenario, they are consistent with previous experience and with the energy, *e*, parameters of Table II. Thus we observe somewhat larger ${}^{L}t_{\lambda}$ values for thiocyanate than amine than halogen ligations, for both $L = P$ and $F$, and that ${}^{P}t_{\sigma} > {}^{F}t_{\sigma}$ for all.

Recalling that the guesses in Table VIII represent likely minima, we see that the relatively small ${}^{L}t_{\lambda}$(Neq) values in Table V are to be seen as reflections of weaker equatorial bonding and overlap than axial: qualitatively, at least, that is supported by the $e_{\sigma}$ values in Table II. This lesser equatorial ligand donation should, according to theory[14,18] and previous experience,[14-19] be reflected in a greater ratio ${}^{F}t_{\lambda}$:${}^{P}t_{\lambda}$ for the equatorial ligands, and this also seems to be confirmed by the values in Tables V and VIII. Further, as the equatorial bonding weakens and so places more bond density nearer the ligand and hence further from the metal and the nature of the operator *er* is such as to amplify the more distant parts of the bond,[18] we can comprehend the larger ${}^{F}t_{\sigma}$(Neq) values for the nickel complex over the cobalt.

Finally, the decreased $\pi$ donor role of the axial X ligators on replacing cobalt by nickel, as discussed in connection with the energy parameters earlier, appears to be reflected also in the smaller $t_{\pi}$ parameters for the nickel halogen chromophores. Again, these parameters appear to have larger *F*:*P* ratios than the corresponding $t_{\sigma}$ parameters, in line with earlier experience.[18]

Altogether, variations in the *t* parameters appear to be consistent with trends in the *e* parameters and geometrical structures, though proof is lacking because of the fundamental impossibility of resolving contributions to intensity from diametrically opposite ligations.

### Circular Dichroism

The differential absorptions of left- and right-handed circularly polarized light for these eight chromophores have been measured by Utsuno et al.[1] and are reproduced in Figure 3. While the experimental frequency range for the absorption spectra extended to ca. 5000 $cm^{-1}$ in the infrared, that for the CD spectra only reached ca. 10000 $cm^{-1}$. Three CD bands are observed for each of the cobalt species, the middle one in each case having virtually no intensity. Four appear in the nickel spectra, although the positive features at ca. 10000 $cm^{-1}$ are incomplete. For the following analyses, these traces have been extended by guesswork as indicated by broken lines. Areas under all CD spectral traces have been estimated once again by cutting out and weighing copies.

Calculation of CD for these solutions entails evaluation of the scalar product of electric- and magnetic-dipole matrix elements, for all transitions occurring within the appropriate band ranges, as described by Schellman.[2] The electric-dipole transition moments are those calculated and parametrized within the foregoing intensity analyses. The corresponding magnetic-dipole matrix elements are evaluated by using the usual magnetic moment operators $\mu_{\alpha} = kl_{\alpha} + 2s_{\alpha}$ ($\alpha = x, y, z$), where $k$ is the orbital reduction factor. As discussed elsewhere,[16] contributions to circular dichroism from the spin angular momentum are of second order only, and although it is not ignored at all within our computations, the calculated CD is virtually proportional to $k$. We have sought to reproduce the experimental rotatory strengths with $k$ values around 0.9, in line with the general experience of this parameter. As for the transition energies and intensities, all CD calculations have been performed within our CAMMAG3 program suite.[21]

Although presented separately here, rotatory strengths were calculated simultaneously with absorption intensities and the results monitored throughout the wide ranges of ${}^{L}t_{\lambda}$ parameters explored there. For no combination of *t* parameters, whether reproducing observed absorption strengths or not, are the experimental CD differential intensities reproduced. Rotatory

**Table IX.** Comparisons between Observed Rotatory Strengths[a] and Those Calculated[d] with the Parameter Sets of Tables II and V Together with the Given Values[b] of $e_{\pi\sigma}(xz)$ for the Equatorial Amine Ligations

| | | CoLNCS | | CoLCl | | CoLBr | | CoLI | |
|---|---|---|---|---|---|---|---|---|---|
| $e_{\pi\sigma}(xz)$ | band | obsd | calcd | obsd | calcd | obsd | calcd | obsd | calcd |
| +50 | 1 | −13 | −12 | −13 | −13 | −13 | −13 | −12 | −12 |
| | 2 | 0 | −0.4 | 0 | −0.2 | 0 | −0.2 | 0 | −0.1 |
| | 3 | −8 | −9 | −10 | −10 | −10 | −10 | −9 | −10 |
| | 4[c] | | −1 | | −2 | | −3 | | −5 |
| | | NiLNCS | | NiLCl | | NiLBr | | NiLI | |
| $e_{\pi\sigma}(xz)$ | band | obsd | calcd | obsd | calcd | obsd | calcd | obsd | calcd |
| +80 | 1 | −17 | −15 | −16 | −16 | −16 | −18 | −16 | −15 |
| | 2 | −10 | −8 | −8 | −8 | −9 | −8 | −10 | −13 |
| | 3 | +7 | +9 | +8 | +8 | +8 | +10 | +10 | +10 |
| | 4[c] | | +4 | | +4 | | +4 | | +4 |

[a] $R_{gn}\nu_{gn}/10^{-37}$ D $\mu_B$ for transitions $g \rightarrow n$. [b] $cm^{-1}$. [c] Not observed—out of instrument range. [d] Orbital reduction factors, $k$: for cobalt species, $k$ = 0.95; for nickel species, $k$ = 0.85.

strengths only 10 times smaller than observed are calculated for the cobalt chromophores. In the nickel systems, the signs of the features at ca. 10000 and ca. 14000 $cm^{-1}$ are reversed, and again, magnitudes are generally calculated an order of magnitude too low.

The reason for these failures is immediately apparent on reference to the molecular structure shown in Figure 1. Natural optical activity only arises in the absence of mirror symmetry in the chromophore, of course. A near-perfect mirror is established by donor atom coordinates to include the atoms N1, N2, M, and X. Such small rotatory strengths as are calculated within the model so far arise, therefore, from the slight imprecision of this mirror plane. Actually, the calculated rotatory strengths of the bands of the cobalt species at ca. 12000 and ca. 18000 $cm^{-1}$ are composed of small contributions from components within each band of opposite sign and nearly equal magnitude.

Ligand-field theory is concerned solely with perturbations of the metal d electrons, and the models employed invariably identify sources for those perturbations in spatial regions close to the central metal. For the reproduction of spectral absorbance, one effectively parametrizes the small admixtures of odd-parity functions into the *d* orbitals. Now the obvious and undoubted origin of chirality in the present species lies in the $\delta\delta\delta$ conformation of the three NCCN chains in the tripod ligand.[1] The question arises as to how the tripod communicates its chirality to the metal d electrons when the donor atom set is itself virtually achiral. We propose that this happens by virtue of local M–N(eq) bent bonding arising out of slight chelate ring strain. Unambiguous evidence of bent bonding and other forms of misdirected valency in other complexes has accrued from several detailed ligand-field studies recently.[10-14,16]

In the present complexes, the coordination by the *S*-tan tripod comprises, in effect, coordination by substituted ethylenediamine chelates. That ligand is well-known for its adaptability toward metal atoms of varying size in complexes of varying coordination number, a facility owed in large measure to the rotational possibilities—though hindered—about the single bonds of its backbone. Nevertheless, it is unreasonable to suppose that all energetic demands in these systems can be satisfied ideally and simultaneously. In particular, one cannot expect, in general, that amine donor orbitals—essentially of $sp^3$ character—are directed exactly toward the metal atom. Departures from that ideal will be of two kinds: the amine donor orbitals may lie in a plane but be directed toward a point in front of, or behind, the metal atom and/or the two donor orbitals may not be directed at same point. Generally we expect such nonideality to be slight, as a result of compromises made by the ethylene chain conformation and, indeed, to be undetectable by many techniques and criteria. Measurement of optical chirality, however, does seem to provide a most sensitive probe of such features. A recent analysis[16] of the absorption and CD spectra of the nominally tetrahedral chromophore, dichloro[(+)-*N*,*N*,*N*′,*N*′-tetramethyl-1,2-propylenediamine]cobalt(II), ascribed the origin of chirality to misdirected valency of both kinds described above. Within the CLF approach, these features are parameterized with cellular, off-diagonal $e_{\pi\sigma}$ parameters in, and perpendicular to, local Co–N–C($H_2$) planes. In that analysis,[16] proper recognition of the bent bonding involved both $e_{\pi\sigma}$ and $e_\pi$ energy parameters for each plane (*xz* and *yz*) together with $^Lt_{\pi x}$ and $^Lt_{\pi y}$ intensity parameters. Although unique values for all these parameters could not be supported by the available data, combinations of nonzero values for all were necessary. Typical values for the $e_{\pi\sigma}$ parameters were ca. 500 $cm^{-1}$.

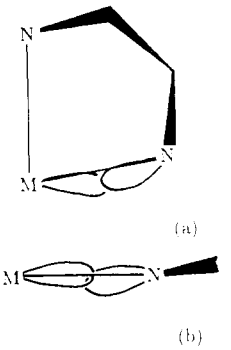


**Figure 4.** Misdirection of the metal and amine orbitals occurring in two planes: (a) side view; (b) top view.

A similar extension of the *e* and *t* parameter sets for the present *S*-tan chromophores with their smaller data bases obviously presented a dismal prospect. By way of an initial exploratory probe, we investigated the response of the model to inclusion of just $e_{\pi\sigma}$ in the plane of each local M-N-C($H_2$) plane (*xz*). This parametrizes both kinds of bent bonding discussed above because the equatorial M–amine bonds do not lie in these planes; see Figure 4. Again, we emphasize that the use of only $e_{\pi\sigma}(xz)$ represents an incomplete parameter set[15] and hence an averaged account of the bent bonding. However, with all *e* and *t* parameters fixed as determined in the preceding analyses, excellent reproduction of the rotatory strengths of all cobalt chromophores was obtained with $e_{\pi\sigma}(xz)$ values of ca. 50 $cm^{-1}$ and of all nickel ones with $e_{\pi\sigma}(xz)$ = 80 $cm^{-1}$. Small variations in these values still provide quantitative reproduction of the experimental CD spectral intensities provided they are accompanied by corresponding adjustments in the orbital reduction factor, *k*. In an alternative approach, the effects of bent bonding were parametrized by inclusion of only $^Pt_{\pi x}$ and $^Ft_{\pi x}$ intensity parameters. Similarly good reproduction of the CD experiment is obtainable for values of these parameters of about 1–2 for the cobalt species, and 2–3 for the nickel ones, relative to the *t* parameter values of Table V. Similar remarks about correlations with *k* apply. The quality of typical examples of these fits is shown in Table IX.

### Geometry in Chirally Chelated Complexes

Remarkably consistent analyses of both frequencies and absorption strengths of the "d–d" transitions throughout this series of eight chromophores have emerged, not only with respect to the

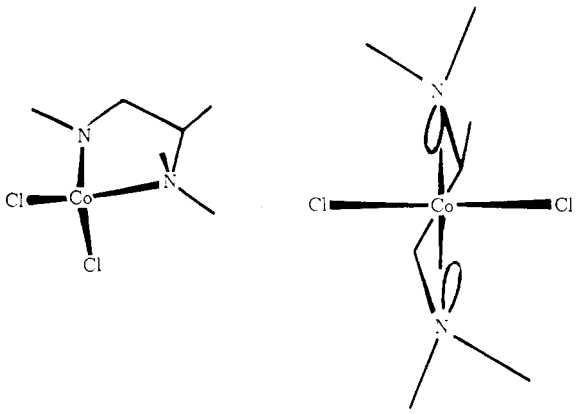


**Figure 5.** Coordination geometry in the pseudotetrahedral chromophore dichloro[(+)-*N,N,N',N'*-tetramethyl-1,2-propylenediamine]cobalt(II).

**Table X.** Angles (deg) Subtended at Nitrogen Donor Atoms (See Figure 6)

| complex | λ | μ | ν | $\bar{\nu}$ |
|---|---|---|---|---|
| Co(*S*-tan)Br[a] | 113 | 111 | 109 | |
| | 113 | 110 | 103 | 108 |
| | 113 | 112 | 111 | |
| Co($Me_6$tren)Br[b] | 115 | 111 | 109 | 109 |
| Ni($Me_6$tren)Br[b] | 114 | 109 | 104 | 104 |
| Co(prop)$Cl_2$[a,c] | 111 | 107 | 102 | 103 |
| | 112 | 109 | 105 | |

[a] Different values for symmetry-unrelated sites. [b] Molecular 3-fold symmetry. [c] prop = *N,N,N',N'*-tetramethyl-1,2-propylenediamine—see Figure 5.

smooth variations in *e* and *t* ligand-field parameter values but also in terms of correlations with the d-electron distribution and with detailed coordination geometry. While equally quantitative reproduction of the experimental CD rotatory strengths has been possible, it is unfortunate that only semiquantitative estimates of the parameters for bent bonding have emerged. Nevertheless, it is possible to correlate these estimates with further geometric details of the molecular structures. Before doing so, we remark that neither calculated frequencies nor intensities are significantly altered by the inclusion of the small $e_{\pi\sigma}$ or $t_\pi$ parameters that permit reproduction of the CD also.

It is illuminating to compare the CD, bent-bonding parameters, and X-ray structural details not only of the *S*-tan complexes and their $Me_6$tren analogues but also of the tetrahedral propylenediamine complex[16] mentioned earlier and shown in Figure 5. In Table X, and the associated Figure 6, are collected angles around the donor amine nitrogens atoms (those in equatorial sites for the trigonal bipyramids: those for both (equivalent) sites in the tetrahedral complex) that illustrate the slight departures of the orientations of ideal N $sp^3$ hybrids from the appropriate M–N vector. Taken individually, many of the deviations from 109° or from appropriate equivalence are barely, if at all, statistically significant. As a group, however, one can discern two consistent features. First, differences between M–N–Me angles, $|\lambda - \mu|$, are very slight for the *S*-tan and $Me_6$tren cobalt complexes but a little larger for the nickel trigonal bipyramid, as also for the tetrahedral cobalt complex. These differences are some measure of the twist distortion that describes amine hybrids as directed at different points. Secondly, the chelate angles M–N–$C(H_2)$, ν, tend to decrease along the series cobalt (TBP) > nickel (TBP) > cobalt (tet), suggesting increasing ring strain along that same series.

The trends are clearly very slight and are doubly uncertain in terms of their relevence to the solution CD studies. Considering

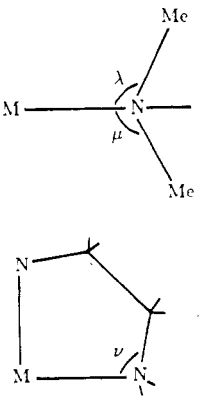


**Figure 6.** Labeling angles given in Table X.

the cobalt and nickel trigonal bipyramids, we note the very small rotatory strengths observed ($\Delta\epsilon/\epsilon$ ratios are ca. $1.2 \times 10^{-3}$) and that very small $e_{\pi\sigma}$ values (or equivalent) are sufficient to account for them. However, we have also observed that somewhat larger values for $e_{\pi\sigma}$ are favored for the nickel species relative to the cobalt: this qualitatively correlates with the slightly greater ring strain that is apparent in the nickel complexes. Clearly, the CD experiment is a most sensitive probe of such bonding details. Then recall that, for the tetrahedral propylenediamine chromophore, $e_{\pi\sigma}$ values of ca. 500 $cm^{-1}$ were required[16] to reproduce those rotatory strengths. The relatively large difference between the trigonal-bipyramidal and tetrahedral systems nicely confirms our earlier proposals[16] concerning the bent bonding in the four-coordinate molecule. Thus, the bond orbitals will tend to be tetrahedrally arranged close to the metal atom but oriented at right angles in the trigonal bipyramidal (so far as the axial and equatorial tripod donor sites are concerned). The angular mismatch between the demands of the metal (interelectron repulsions) and those of the chelate is thus greater for the tetrahedral complex. The M–N bonds are more bent in that system, and the greater value of $e_{\pi\sigma}$ monitors this.

## Summary

The empirical ability of ligand-field theory to reproduce "d–d" (or "f–f") transition energies, paramagnetic susceptibilities, and ESR g values in hundreds of transition-metal complexes witnesses a long-standing success. The development of superpositional models, first the angular overlap model and then the cellular ligand-field approach, has extended the utility of ligand-field theory beyond the mere reproduction of experiment to correlation with bonding and chemical functionality. Earlier commentary on individual σ and π bonding has been supplemented by an increasing number of studies that demonstrate, unambiguously, the role of bent bonding and other forms of misdirected valency. All these achievements have now been repeated and refined by the reproduction of "d–d" absorption strengths and, lately, of rotational strengths determined by CD measurements. Computation of all these properties is carried out within appropriate bases of free-ion $d^n$ configurations. While the studies attest to the continuing relevance and applicability of the ligand-field method, the main achievements of these studies is surely their provision of direct and pictorial chemical bonding understanding. That is owed to the physicality which is built into the superpositional approach. We suggest that the future design of chiral chromophores, for example, might benefit from closer scrutiny of the primary coordination shells in transition-metal complexes.

**Acknowledgment.** N.D.F. acknowledges the award of an SERC studentship.